

# Role of Mixing in Copolymerizations of Styrene and *n*-Butyl Acrylate

E. ÖZDEĞER, E. D. SUDOL, M. S. EL-AASSER, A. KLEIN

Emulsion Polymers Institute and Department of Chemical Engineering, Lehigh University, Bethlehem, Pennsylvania 18015

Received 8 December 1997; accepted 23 January 1998

**ABSTRACT:** The effect of agitation speed and impeller type on the kinetics of emulsion copolymerization of styrene and *n*-butyl acrylate was investigated. It was shown that the solids content was an important variable in these studies. At low solids (30%), the impeller type and speed did not have any significant effect on the final number of particles and the overall rate of polymerization. Particle size distributions were unimodal in all the cases. At high solids (50%), some differences were observed when 2 different impellers (Rushton and A310 fluidfoil) were used. The polymerization carried out with the Rushton impeller was faster. Bimodal particle size distributions were obtained for both cases; however, the bimodality was more significant when the A310 fluidfoil impeller was used. Greater numbers of particles and unimodal particle size distributions with high rates of polymerization at 30% solids contrasted the lower numbers of particles and bimodal particle size distributions with lower rates of polymerization seen at 50% solids. These differences were attributed to the partitioning behavior of the surfactant (Triton X-405; octylphenoxy polyethoxy ethanol; Union Carbide, Danbury, CT). © 1998 John Wiley & Sons, Inc. *J Appl Polym Sci* 69: 2277–2289, 1998

**Key words:** emulsion copolymerization; mixing; styrene; *n*-butyl acrylate; nonionic surfactant; Triton X-405

## INTRODUCTION

In emulsion polymerization, mixing can play a significant role in determining the kinetics of the polymerization. In addition to maintaining a uniform temperature throughout the reactor, it controls the degree of dispersion of the immiscible oil (monomer) phase in the continuous aqueous medium. This is important throughout roughly the first half of the reaction, in which monomer droplets serve as reservoirs supplying the monomer by diffusion to the growing (polymerizing) submicron polymer particles. Too little agitation leads to large droplets and phase separation, which may result in diffusion limitations in sys-

tems in which the monomer is sparingly water-soluble. On the other hand, too much agitation can lead to either reduced nucleation of particles or nucleation in the monomer droplets. The stability of the particles as manifested by coagulum formation can also be dependent on the shear to which the latex is subjected during various phases of the reaction.

The effect of agitation on the kinetics of emulsion polymerization is an area that has not been reported upon a great deal in the open literature. One reason for this may be the conflicting results obtained by various researchers. Scunmukham et al.<sup>1</sup> showed a negative effect of violent agitation on the rate of polymerization, whereas Schoot et al.<sup>2</sup> contradicted this result. On the other hand, Omi et al.<sup>3</sup> showed that in preparing the emulsion, increasing the agitation intensity decreased the polymerization rate; but once it was prepared under specific conditions, there was no effect of

---

Correspondence to: A. Klein.

stirring on the emulsion polymerization of styrene over the range studied (200–700 rpm). Nomura et al.<sup>4</sup> and Rollin et al.<sup>5</sup> found an optimum range of stirring speed (410–600 rpm) over which styrene polymerizations were unaffected over the entire reaction. The effect of stirrer speed (300 versus 500 rpm) on the emulsion polymerizations of styrene was also studied by Varela de la Rosa.<sup>6</sup> He found that below the critical micelle concentration (CMC), the rate of polymerization decreased with increasing stirrer speed; whereas above the CMC, its effect was insignificant. Also, the emulsion polymerization of vinylidene chloride was studied by Evans et al.,<sup>7</sup> and for the three intervals of emulsion polymerization, three different observations were made. In interval I, a decrease in the polymerization rate was observed with an increase in the stirrer speed (0–756 rpm). This was followed by an increase in the polymerization rate in interval II with increasing stirrer speed (0–400 rpm), while the polymerization rate in interval III was independent of the stirrer speed. For vinyl acetate, 2 conflicting results were reported by Zollars<sup>8</sup> and Stannett et al.,<sup>9</sup> with Zollars showing no significant effect of agitation on the reaction rate, while Stannett et al. concluded that there were significant differences. Recently, Bataille et al.<sup>10</sup> studied the effect of agitation on vinyl acetate emulsion polymerizations and showed that it had little influence on the rate of polymerization. Also, Weerts et al.<sup>11</sup> showed an increase in rate with increasing stirrer speed for the emulsion polymerization of butadiene.

In this work, the role of mixing is investigated in the copolymerization of styrene and *n*-butyl acrylate. The effect of agitation speed (400 and 1000 rpm) on the kinetics of the polymerizations and the number of particles is studied. The evolution of the copolymer composition is followed with respect to conversion. To determine the effect of impeller type, results are compared for 2 impellers (A310 fluidfoil and Rushton). Solids content is another variable studied; kinetic results are coupled with particle number data and final latex particle size distributions for polymerizations carried out at 30 and 50% solids, and comparisons are made for both impellers.

## EXPERIMENTAL

### Materials

Styrene monomer (Aldrich, Milwaukee, WI), *n*-butyl acrylate monomer (Aldrich), Triton X-

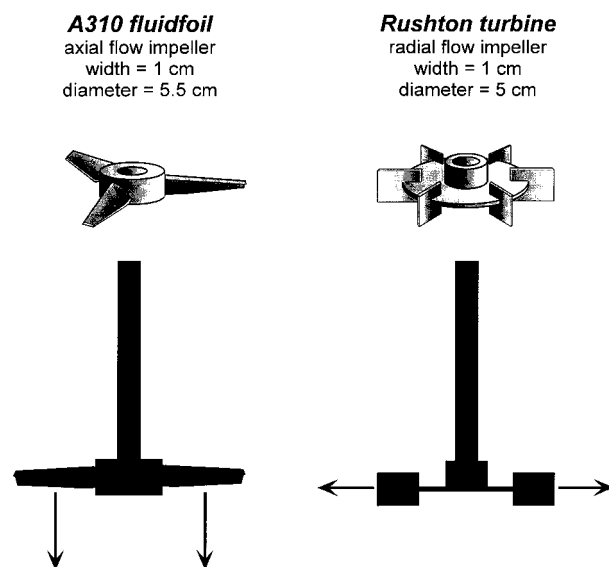


**Figure 1** Schematics of A310 fluidfoil and Rushton impellers.

405 (Union Carbide), and potassium persulfate (Fisher, Fair Lawn, NJ) were all used as received. Distilled–deionized water (DDI) was used in all polymerizations.

### Polymerizations

All copolymerizations of styrene and *n*-butyl acrylate were carried out in a 1-L medium-pressure reactor (MP10) using the Mettler RC1 reaction calorimeter. The reactions were conducted in the isothermal mode at 70°C. Two different impellers were used: A310 fluidfoil and Rushton (Mixing Equipment Co., Rochester, NY). A schematic of the impellers with their dimensions and the direction of flow are given in Figure 1. The Rushton impeller was used with a baffle, whereas for the A310 fluidfoil, the baffle was removed due to the phase separation of the monomers noted when it was initially used. The dimensions of the MP10 reactor and the position of the impeller in the reactor are shown in Figure 2. The polymerizations of styrene and *n*-butyl acrylate were carried out at 400 and 1000 rpm. The polymerization recipes for 30 and 50% solids are given in Table I. In order to compare the effect of solids content in these mixing studies, the amount of surfactant based on the oil phase and the amount of initiator based on the aqueous phase were kept constant at the 2 solids' contents.

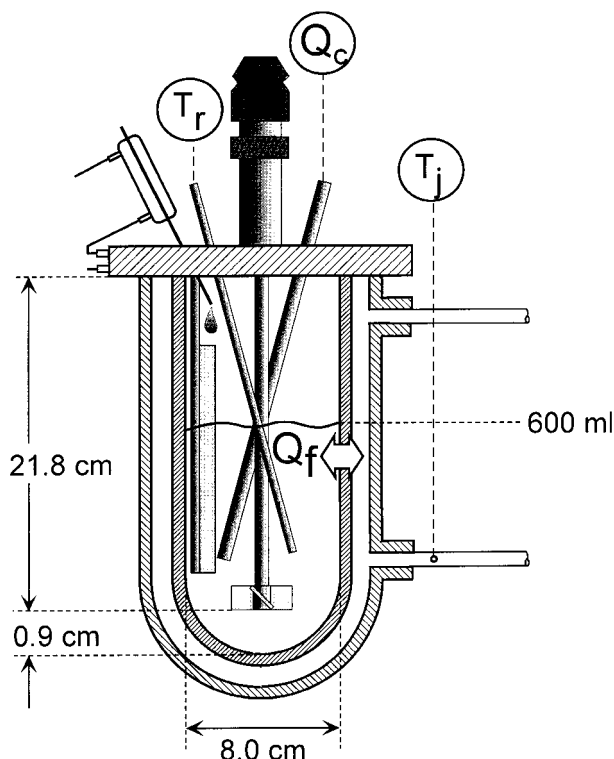


Figure 2 Dimensions of the MP10 reactor.<sup>12</sup>

### Calorimetry

The heat of reaction,  $Q_{\text{rxn}}$ , which is proportional to the rate of polymerization, is obtained by the energy balance for the calorimeter and is given by the following equation:

$$Q_{\text{rxn}} + Q_{\text{stirrer}} + Q_{\text{calibration}} = Q_{\text{flow}} + Q_{\text{accumulated}} + Q_{\text{loss}} \quad (1)$$

In eq. (1),  $Q_{\text{stirrer}}$  is the power input by the stirrer;  $Q_{\text{calibration}}$  is the heat of calibration, which for a reaction, drops out of the equation (no calibration is run during a reaction);  $Q_{\text{flow}}$  is the heat flow through the reactor wall to the cooling system;  $Q_{\text{accumulated}}$  is the heat accumulated in the reaction system; and  $Q_{\text{loss}}$  is the heat loss to the surroundings.  $Q_{\text{stirrer}}$  and  $Q_{\text{loss}}$  are considered in the baseline of the process ( $Q_{\text{baseline}} = Q_{\text{stirrer}} - Q_{\text{loss}}$ ), and the  $Q_{\text{flow}}$  and  $Q_{\text{accumulated}}$  terms are given in eq. (2) and (3), respectively.

$$Q_{\text{flow}} = UA(T_r - T_j) \quad (2)$$

$$Q_{\text{accumulated}} = (mc_p)_T dT_r/dt \quad (3)$$

$U$  is the overall heat transfer coefficient ( $\text{W}/\text{m}^2\text{C}$ ),

$A$  is the heat exchange area ( $\text{m}^2$ ),  $T_r$  and  $T_j$  are the reactor and jacket temperatures ( $^{\circ}\text{C}$ ), respectively, and the  $(mc_p)_T$  term includes the mass and the heat capacities of the reaction system and the inserts (temperature sensor, impeller, shaft, etc.). In calculating  $Q_{\text{rxn}}$ , the temperature in the reactor and in the jacket are assumed to be homogeneous, the reaction mixture is considered to be perfectly mixed, and the changes in kinetic and potential energies are assumed to be negligible. By rearranging eq. (1) and substituting eq. (2) and (3), one obtains

$$Q_{\text{rxn}} = UA(T_r - T_j) + (mc_p)_T dT_r/dt - Q_{\text{baseline}} \quad (4)$$

Further details about the use of the Mettler RC1 reaction calorimeter in monitoring emulsion polymerizations can be found in the work of Varela de la Rosa et al.<sup>13</sup>

Equation (5) defines the overall calorimetric conversion,  $X_c$ , for copolymerization reactions:

$$X_c = \frac{M_A(-\Delta H_A) + M_B(-\Delta H_B)}{M_{AO}(-\Delta H_A) + M_{BO}(-\Delta H_B)} = \frac{\int_0^t Q_{\text{rxn}} dt}{M_{AO}(-\Delta H_A) + M_{BO}(-\Delta H_B)} \quad (5)$$

where  $M_i$ ,  $M_{i0}$ , and  $\Delta H_i$  are the moles of monomer  $i$  reacted, the initial moles of monomer  $i$ , and the heat of homopolymerization ( $\text{kJ}/\text{mol}$ ; the negative sign indicates that the reaction is exothermic),

Table I Recipe for Emulsion Copolymerizations of Styrene and *n*-Butyl Acrylate

Ingredient	Amount (g)	
	30% Solids	50% Solids
Styrene	91.79	150.00
<i>n</i> -Butyl acrylate	91.79	150.00
Triton X-405 <sup>a</sup> (70%)	21.01 <sup>b</sup>	34.30 <sup>d</sup>
Distilled-deionized water	425.20	289.72
Potassium persulfate	1.7260 <sup>c</sup>	1.2000 <sup>e</sup>

<sup>a</sup> Octyl phenoxy polyethoxy ethanol (average of 40 ethylene oxide units per molecule; Union Carbide; CMC = 0.86 mM), 30% water.

<sup>b</sup> 35.2 and 16.6 mM based on oil and aqueous phases, respectively.

<sup>c</sup> 14.8 mM based on the aqueous phase.

<sup>d</sup> 35.2 and 39.1 mM based on oil and aqueous phases, respectively.

respectively. In eq. (5), the heat of crosspropagation is assumed to be equal to the heat of homopolymerization. Urretabizkaia et al.<sup>14</sup> have shown that this is a good approximation in batch emulsion copolymerizations of methyl methacrylate-*n*-butyl acrylate, vinyl acetate-*n*-butyl acrylate, and methyl methacrylate-vinyl acetate.

On the other hand, the overall gravimetric conversion is given as follows:

$$X_g = \frac{M_A MW_A + M_B MW_B}{M_{AO} MW_A + M_{BO} MW_B} \quad (6)$$

where  $MW_i$  represents the molecular weight of monomer  $i$ . Comparing eq. (5) and (6), one can see that calorimetric and gravimetric conversions would only be equal if  $\Delta H_A/\Delta H_B = MW_A/MW_B$ , and this is not the case for styrene and *n*-butyl acrylate ( $\Delta H_A/\Delta H_B = 0.94$ ;  $MW_A/MW_B = 0.81$ , where  $A$  is styrene and  $B$  is *n*-butyl acrylate). Therefore,  $X_c$  and  $X_g$  cannot be compared directly for these copolymerization reactions.

### Characterization

The overall conversions were determined gravimetrically. The samples were dried to constant weight in an oven at 65°C. Capillary hydrodynamic fractionation (CHDF) (Model 1100, Matec Applied Sciences, Northborough, MA) was used to determine the latex particle size and particle size distributions.

Copolymer composition was determined using gas chromatography (HP 5890A). Separate calibration curves were prepared for styrene and *n*-butyl acrylate. The monomers were dissolved in methanol. Butanol was added as the internal standard. The area ratio of the monomer to butanol was plotted against their weight ratios. The latex samples were diluted with DDI water to ~2%. A known amount of butanol was added to each sample. Using the calibration curves, the amount of unreacted monomer (for example,  $B$ ) was determined as follows:

$$x = \frac{M_{to} - B \left[ 1 + \frac{A/\text{BuOH}}{B/\text{BuOH}} \right]}{M_{to}} \quad (7)$$

where  $x$  is the overall gravimetric conversion,  $A/\text{BuOH}$  and  $B/\text{BuOH}$  are the weight ratios of each monomer to butanol (obtained from the calibra-

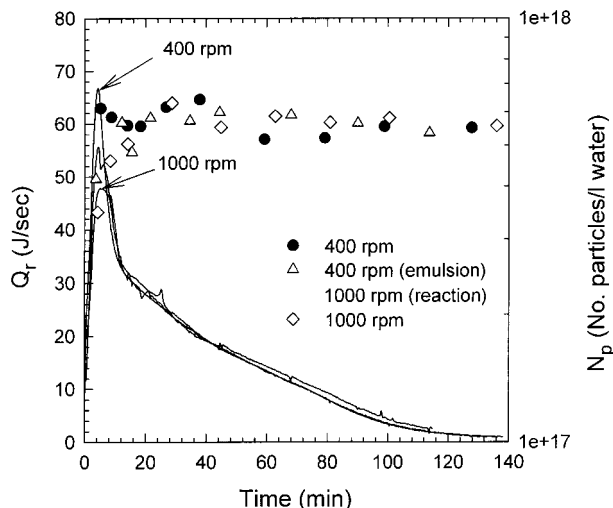


**Figure 3** Heat of reaction ( $Q_r$ , lines) and evolution of number of particles ( $N_p$ , ●, △, ◇) with respect to time as a function of impeller speed for the batch emulsion copolymerizations of styrene and *n*-butyl acrylate (1/1 weight ratio) using the A310 fluidfoil impeller; 30% solids;  $T_r = 70^\circ\text{C}$ .

tion curves), and  $M_{to}$  is the total initial amount of monomers.

Optical microscopy (Bauch and Lomb Optical Co. Model CL25) was used for determining the monomer droplet size in some cases. A sample from the reactor was taken just before the addition of the initiator. It was put on a slide with a cover slip and observed under the microscope. Several micrographs were obtained, and about 500 droplets were counted for each case.

## RESULTS AND DISCUSSION

### Effect of Impeller Speed

As stated above, emulsion copolymerizations of styrene and *n*-butyl acrylate were carried out at 400 and 1000 rpm using the A310 fluidfoil and Rushton impellers and a 30% solids recipe. Figures 3, 4, and 5 show the effect of impeller speed on the heat of reaction and particle number profile, overall conversion, and copolymer composition, respectively, for the A310 fluidfoil impeller. Note that a third reaction was carried out in which the emulsion was prepared at 400 and the impeller speed was increased to 1000 rpm just before the addition of the initiator. The purpose of this experiment was to determine whether the emulsification speed had any effect on the kinetics

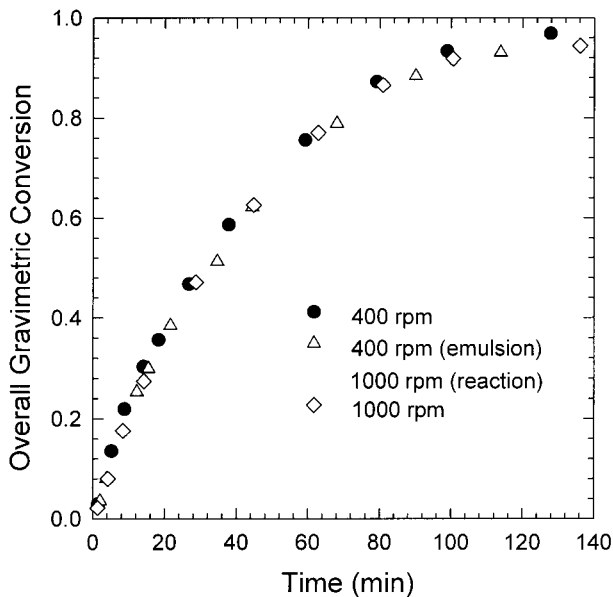


**Figure 4** Overall gravimetric conversion with respect to time as a function of impeller speed for the batch emulsion copolymerizations of styrene and *n*-butyl acrylate (1/1 weight ratio) using the A310 fluidfoil impeller; 30% solids;  $T_r = 70^\circ\text{C}$ .

of polymerization if everything else was kept the same. Looking at Figure 3, one can see that as the impeller speed increased, the initial number of particles, and, thus, the initial rate of polymerization decreased. Note that this distinction cannot be made merely by examining the gravimetric data in Figure 4. In the case in which the emulsification and polymerization speeds were 400 and 1000 rpm, respectively, an in-between behavior was observed. The decrease in the initial number of particles and, therefore, the decrease in the initial rate with increasing impeller speed are expected since smaller and correspondingly higher numbers of monomer droplets are created at higher speeds. This leads to a greater amount of surfactant being adsorbed at the surface of the monomer droplets. Therefore, the amount of surfactant available in the aqueous phase for nucleating particles is lower, leading to a lower initial number of particles. The monomer droplet size distributions are presented in Figure 6. As can be seen, the average droplet size produced using the A310 fluidfoil impeller at 1000 rpm ( $5\ \mu\text{m}$ ) is significantly smaller than that produced at 400 rpm ( $15\ \mu\text{m}$ ).

In these polymerizations, the nucleation of the latex particles seems to end at around 20 min for all the cases, although some scatter is observed for the polymerization carried out at 400 rpm.

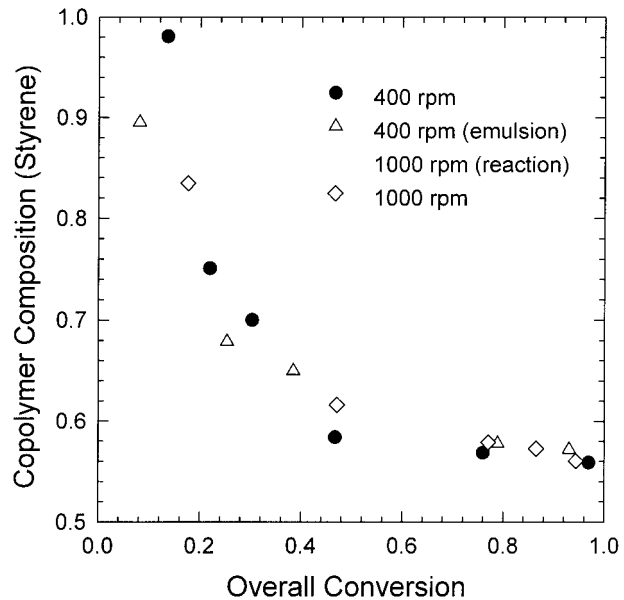


**Figure 5** Evolution of copolymer composition (molar) with respect to overall gravimetric conversion as a function of impeller speed for the batch emulsion copolymerizations of styrene and *n*-butyl acrylate (1/1 weight ratio) using the A310 fluidfoil impeller; 30% solids;  $T_r = 70^\circ\text{C}$ .

This time corresponds to 36–40% conversion (see Fig. 4). In Figure 3, one can see that the heat of reaction (proportional to the rate of polymeriza-

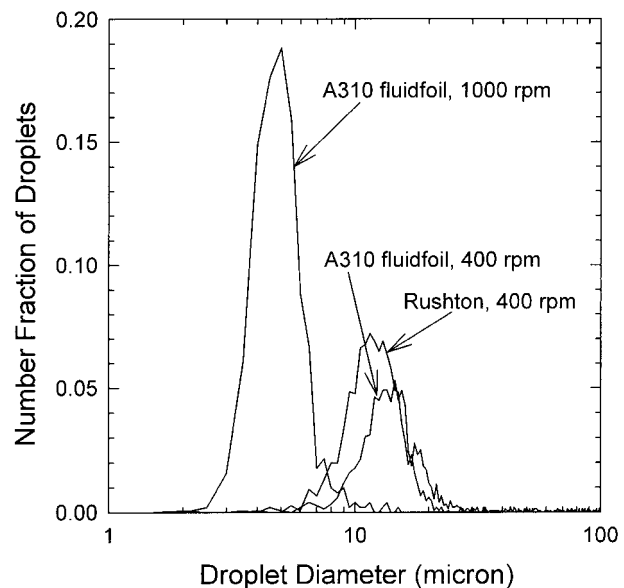


**Figure 6** Comparison of monomer droplet size distributions for the A310 fluidfoil impeller (400 and 1000 rpm) and the Rushton impeller (400 rpm) for the batch emulsion copolymerizations of styrene and *n*-butyl acrylate (1/1 weight ratio) at 30% solids;  $T_r = 70^\circ\text{C}$ .

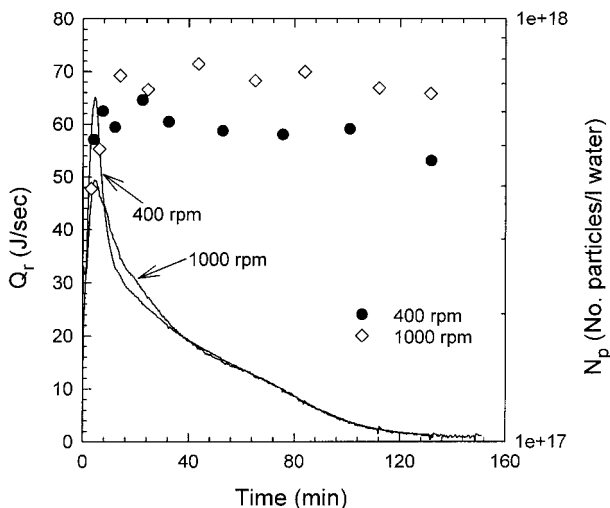


**Figure 7** Heat of reaction ( $Q_r$ , lines) and evolution of number of particles ( $N_p$ , ●, ◇) with respect to time as a function of impeller speed for the batch emulsion copolymerizations of styrene and *n*-butyl acrylate (1/1 weight ratio) using the Rushton impeller; 30% solids;  $T_r = 70^\circ\text{C}$ .

tion) reaches a maximum at around 8 min ( $\sim 20\%$  conversion) and then decreases. Since the decrease in rate occurs at such early conversions, this indicates that there is some limited aggregation during the reaction at early conversions rather than this marking the disappearance of the monomer droplets. This argument is supported by the apparent corresponding decrease in the number of particles for the polymerization carried out at 400 rpm. However, for the other 2 polymerizations, there is not enough data to confirm this. It is seen that the final numbers of particles are very similar for the 3 cases studied. All latex particle size distributions were unimodal.

When one looks at the copolymer composition evolution with respect to conversion (Fig. 5), it is seen that although there are some differences in the copolymer compositions obtained at the various impeller speeds, these are not considered to be significant. In all the cases, the polymer was initially rich in styrene. This is expected since the reactivity ratio of styrene is much higher than that of *n*-butyl acrylate ( $r_{\text{styrene}} = 0.75$ ;  $r_{\text{butyl acrylate}} = 0.20$ ).<sup>15</sup>

The effect of impeller speed on emulsion copolymerizations of styrene and *n*-butyl acrylate was also studied using the Rushton impeller. The heat of reaction and the evolution of the number of particles, overall gravimetric conversion, and copolymer composition are presented in Figures 7, 8, and 9, respectively, for 400 and 1000 rpm. As

seen in the case using the A310 fluidfoil impeller, as the impeller speed increased, the initial number of particles, and, thus, the rate of polymerization decreased (Fig. 7). After the initial period, the rates at the 2 impeller speeds are similar. The number of particles seems to be a little higher for the case in which the impeller speed was 1000 rpm; however, this difference is not considered to be significant enough to conclude that the impeller speed affects the number of particles. More experiments are required to verify this. Looking at the overall conversion and the copolymer composition (Fig. 8 and 9), one can see that they are very similar to each other. Again, the copolymer is initially richer in styrene due to its higher reactivity ratio. The preceding results are for polymerizations carried out at 30% solids. For 50% solids, when the polymerizations were carried out below 1000 rpm, phase separation occurred for both impellers; therefore, impeller speed was not a variable in the high solids content polymerizations.

#### Effect of Impeller Type

Comparisons of the preceding polymerizations were also made in terms of impeller type at a specific impeller speed. Figures 10–12 show the effect of impeller type on emulsion copolymeriza-

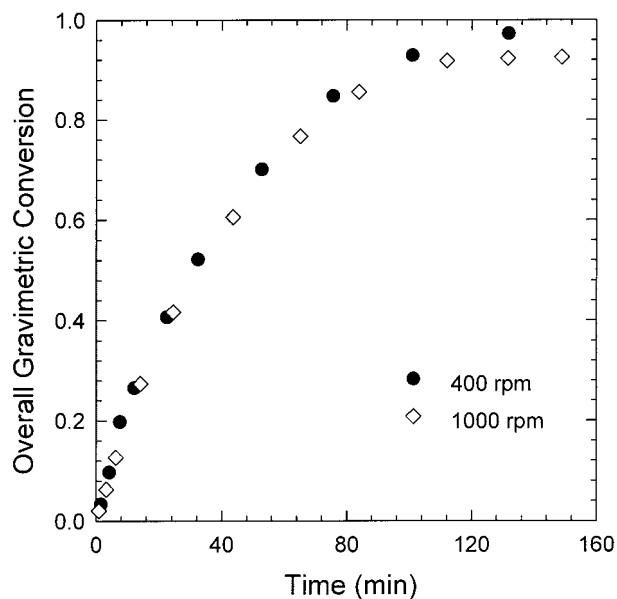


**Figure 8** Overall gravimetric conversion with respect to time as a function of impeller speed for the batch emulsion copolymerizations of styrene and *n*-butyl acrylate (1/1 weight ratio) using the Rushton impeller; 30% solids;  $T_r = 70^\circ\text{C}$ .

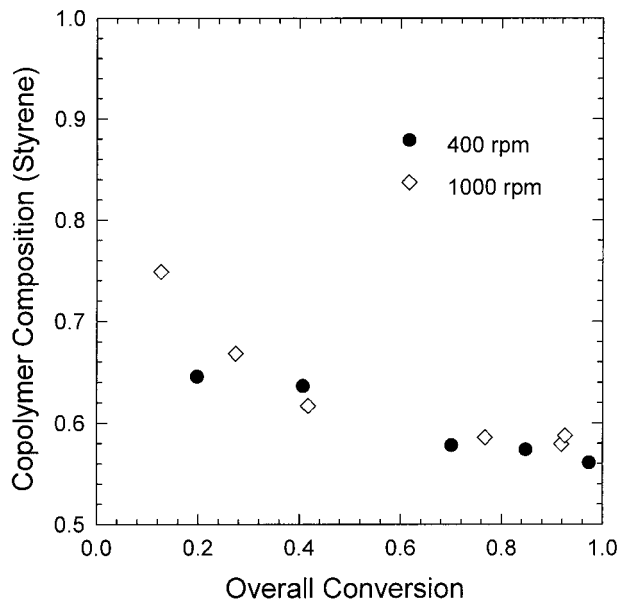


**Figure 9** Evolution of copolymer composition (molar) with respect to overall gravimetric conversion as a function of impeller speed for the batch emulsion copolymerizations of styrene and *n*-butyl acrylate (1/1 weight ratio) using the Rushton impeller; 30% solids;  $T_r = 70^\circ\text{C}$ .

tions of styrene and *n*-butyl acrylate carried out at 400 rpm in terms of heat of reaction and number of particles, overall conversion, and copolymer composition, respectively. The same profiles are

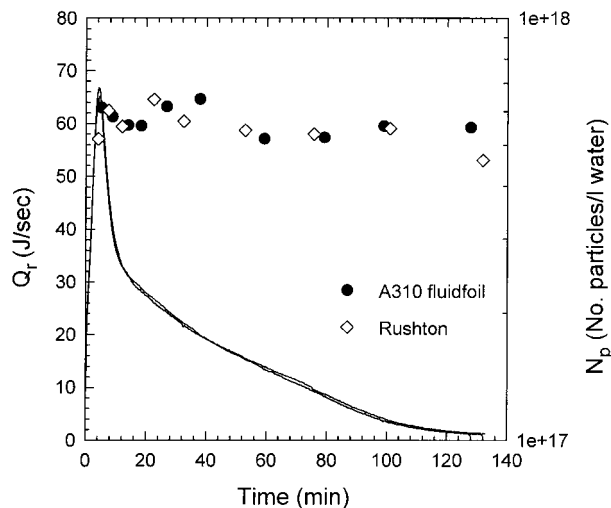


**Figure 10** Heat of reaction ( $Q_r$ , lines) and evolution of number of particles ( $N_p$ , ●, ◇) with respect to time as a function of impeller type for the batch emulsion copolymerizations of styrene and *n*-butyl acrylate (1/1 weight ratio); 400 rpm; 30% solids;  $T_r = 70^\circ\text{C}$ .

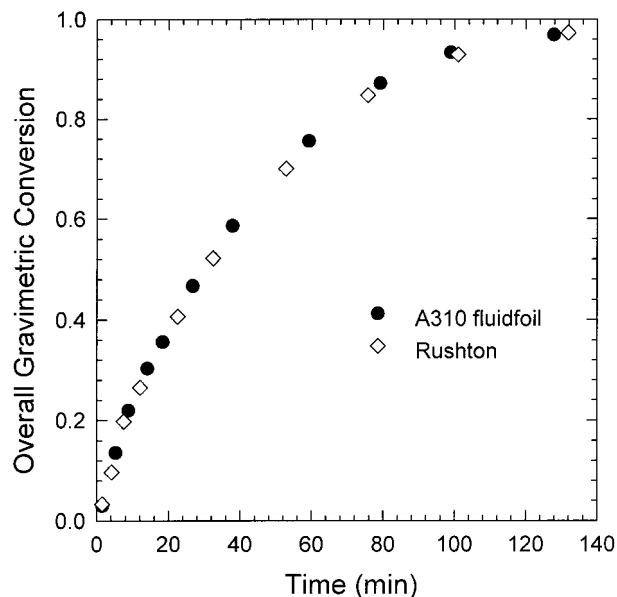


**Figure 11** Overall gravimetric conversion with respect to time as a function of impeller type for the batch emulsion copolymerizations of styrene and *n*-butyl acrylate (1/1 weight ratio); 400 rpm; 30% solids;  $T_r = 70^\circ\text{C}$ .

given in Figures 13–15 for the polymerizations carried out at 1000 rpm. From these figures, one can see that impeller type does not affect the ki-

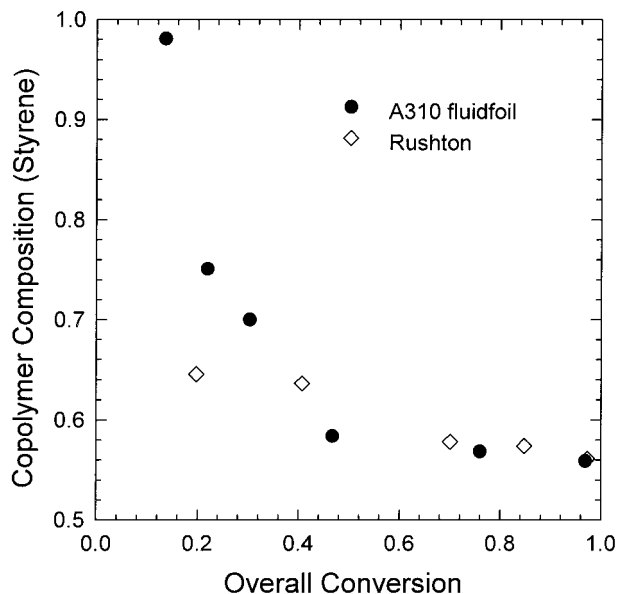


**Figure 12** Evolution of copolymer composition (molar) with respect to overall gravimetric conversion as a function of impeller type for the batch emulsion copolymerizations of styrene and *n*-butyl acrylate (1/1 weight ratio); 400 rpm; 30% solids;  $T_r = 70^\circ\text{C}$ .

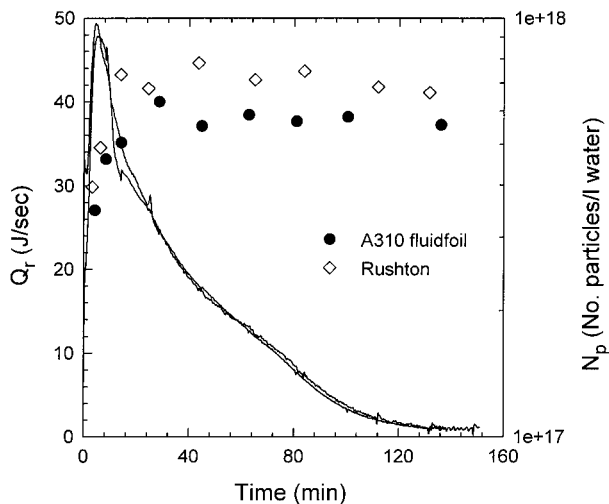


**Figure 13** Heat of reaction ( $Q_r$ , lines) and evolution of number of particles ( $N_p$ , ●, ◇) with respect to time as a function of impeller type for the batch emulsion copolymerizations of styrene and *n*-butyl acrylate (1/1 weight ratio); 1000 rpm; 30% solids;  $T_r = 70^\circ\text{C}$ .

netics of these polymerizations. There are slight differences in the particle number data at 1000 rpm (see Fig. 13) and some deviation in the copolymer composition at the early stages of the polymerization ( $\sim 20\%$  conversion) at 400 rpm

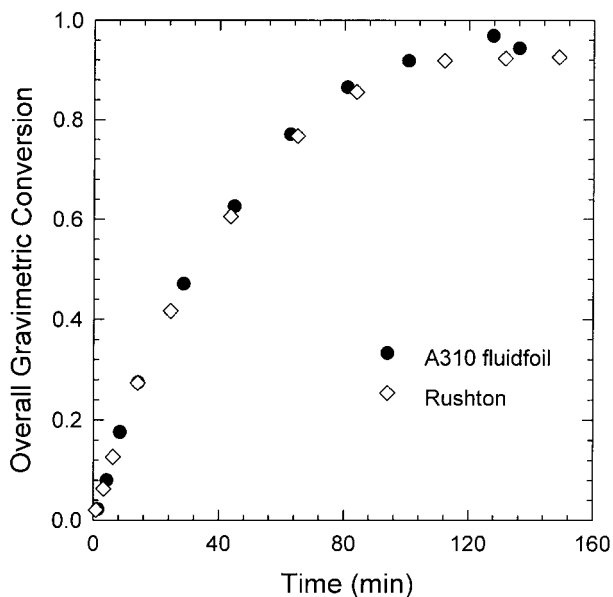


**Figure 14** Overall gravimetric conversion with respect to time as a function of impeller type for the batch emulsion copolymerizations of styrene and *n*-butyl acrylate (1/1 weight ratio); 1000 rpm; 30% solids;  $T_r = 70^\circ\text{C}$ .

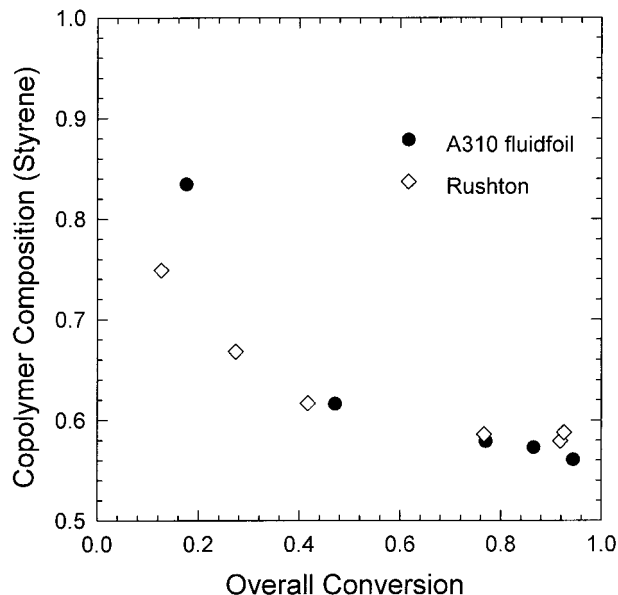


**Figure 15** Evolution of copolymer composition (molar) with respect to overall gravimetric conversion as a function of impeller type for the batch emulsion copolymerizations of styrene and *n*-butyl acrylate (1/1 weight ratio); 1000 rpm; 30% solids;  $T_r = 70^\circ\text{C}$ .

(see Figure 12) for the 2 impellers. However, there are insufficient data to conclude whether these differences are significant.

The polymerizations discussed above were performed at 30% solids. The impeller types were also compared at 50% solids. Figure 16 shows the

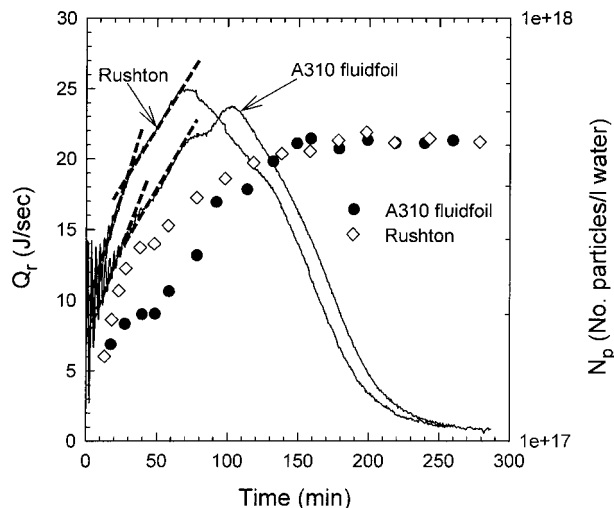


**Figure 16** Heat of reaction ( $Q_r$ , lines) and evolution of number of particles ( $N_p$ , ●, ◇) with respect to time as a function of impeller type for the batch emulsion copolymerizations of styrene and *n*-butyl acrylate (1/1 weight ratio); 1000 rpm; 50% solids;  $T_r = 70^\circ\text{C}$ .



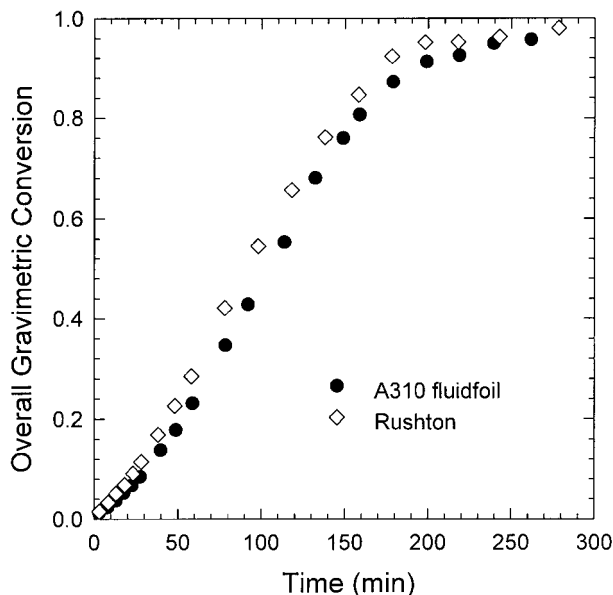


**Figure 17** Overall gravimetric conversion with respect to time as a function of impeller type for the batch emulsion copolymerizations of styrene and *n*-butyl acrylate (1/1 weight ratio); 1000 rpm; 50% solids;  $T_r = 70^\circ\text{C}$ .

heat of reaction profiles and the evolution of the number of particles, and Figure 17 shows the overall conversion with respect to time for the Rushton and A310 fluidfoil impellers at high solids. The initial noise in the heat data is due to the temperature controller. For these polymerizations, the value for the  $p$  parameter [directly related with the degree of temperature control in the reactor;  $T_r - T_j = p(T_r - T_{\text{set}})$ , where  $T_r$  is the reactor temperature,  $T_j$  is the jacket temperature, and  $T_{\text{set}}$  is the temperature set point] was chosen to be 18. The higher the  $p$  parameter (default = 6), the better is the temperature control; however, this tends to produce oscillations in the heat data. For the Rushton impeller, the initial rate is higher than that for the A310 fluidfoil. The rate reaches a maximum around 70 min ( $\sim 38\%$  conversion), then decreases. Up to the maximum in rate, one can see that there are 2 distinct slopes. The slope for the rate is steeper up to  $\sim 30$  min ( $\sim 12\%$  conversion) than that between 30 and 70 min. Also, the increase in the number of particles is faster in the first half-hour. Based on the results of Varela de la Rosa,<sup>16</sup> the initial nucleation period may be attributed to micellar nucleation (greater slope) and the second period to homogeneous nucleation. Although the rate starts decreasing after  $\sim 70$  min ( $\sim 38\%$  conversion), the number of particles continues to increase until

$\sim 150$  min ( $\sim 76\%$  conversion). At 54.5% conversion, the particle size distribution indicates the presence of a second population of particles, which is evident in the skewness in the left side (smaller particle size) of the particle size distribution curve (see Fig. 18). From the results presented in our previous papers,<sup>17-19</sup> it is predicted here that some fraction of the surfactant is solubilized (partitioned) inside the droplets, and as droplets are depleted, this surfactant repartitions to the aqueous phase. Some of it is used for the stabilization of the existing particles, while a portion of it is used for the creation of new particles.

When one looks at the heat profile obtained using the A310 fluidfoil impeller, the same behavior can be observed here as well, although it is not as obvious. There are roughly 2 slopes in rate up to  $\sim 70$  min. The first also lasts the first  $\sim 30$  min ( $\sim 10\%$  conversion), while the second is again between 30 and 70 min ( $\sim 30\%$  conversion). The same interpretation in terms of nucleation mechanisms is offered here as well. However, in contrast to the case where the Rushton impeller was used, between 70 and 90 min, a short, nearly constant, rate period is observed, followed by an increase. In this case, the rate reaches a maximum at around 100 min ( $\sim 48\%$  conversion) and then decreases. The increase in the initial number of particles is not as fast as was the case with the Rushton impeller. At the same time, where the

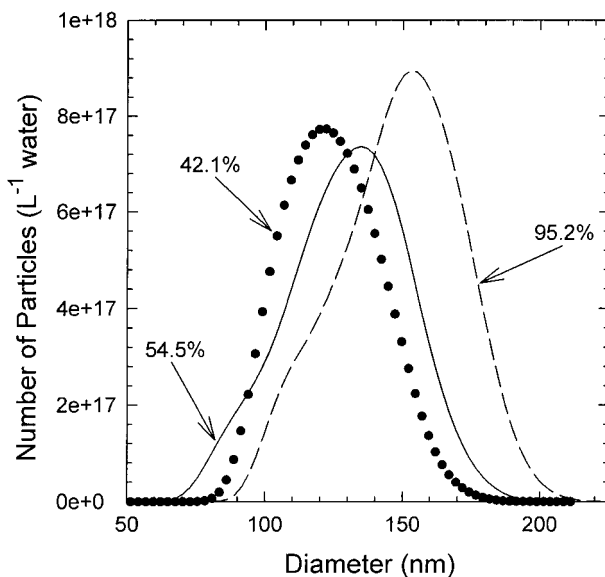


**Figure 18** Evolution of particle size distribution for the batch emulsion copolymerization of styrene and *n*-butyl acrylate (1/1 weight ratio) using the Rushton impeller; 1000 rpm; 50% solids;  $T_r = 70^\circ\text{C}$ .

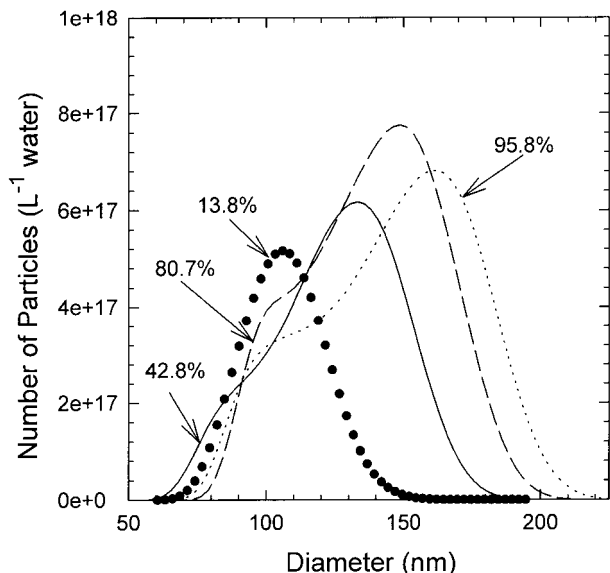


**Figure 19** Evolution of particle size distribution for the batch emulsion copolymerization of styrene and *n*-butyl acrylate (1/1 weight ratio) using the A310 fluidfoil impeller; 1000 rpm; 50% solids;  $T_r = 70^\circ\text{C}$ .

increase in rate occurs ( $\sim 90$  min, 42.8% conversion), the particle size distribution indicates that a second population of particles has formed in this case as well (see Fig. 19). However, compared to the case with the Rushton impeller, this population is more distinct.

When the Rushton and A310 fluidfoil impellers are compared in terms of their mixing characteristics, the Rushton impeller, being a high shear impeller, would be normally expected to give lower initial rates by creating more droplets with a greater surface area, which can adsorb surfactant. However, in the RC1, the impellers are relatively close to the wall of the reactor ( $\sim 1$  cm). Therefore, the A310 fluidfoil impeller might have created more shear at 50% solids and 1000 rpm, which would lead to smaller monomer droplet sizes. This would require more of the surfactant to be associated with the oil phase, which will cause the lower initial number of particles. As the droplets are consumed, there would be more surfactant available for the creation of new particles after stabilization of the existing ones. The presence of a more distinct second population of particles may be the result of having more available surfactant in the later stages of the polymerization when the A310 fluidfoil was used.

#### Effect of Solids Content

The polymerizations that were carried out 1000 rpm were compared at 30 and 50% solids using

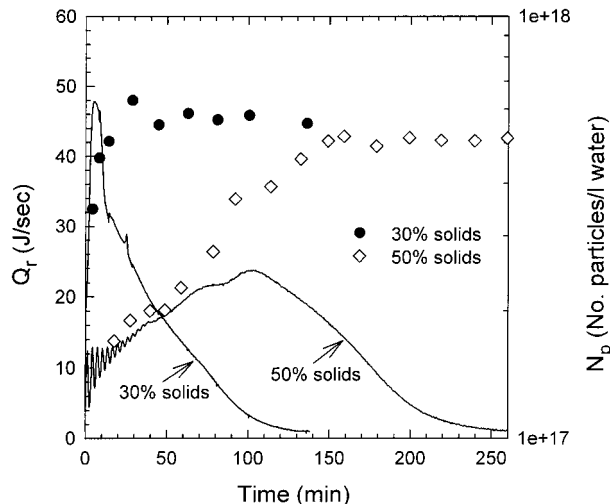


**Figure 20** Heat of reaction ( $Q_r$ , lines) and evolution of number of particles ( $N_p$ , ●, ◇) with respect to time as a function of solids content for the batch emulsion copolymerizations of styrene and *n*-butyl acrylate (1/1 weight ratio); 1000 rpm; A310 fluidfoil impeller;  $T_r = 70^\circ\text{C}$ .

both impellers to see whether the solids content has an effect in studying the role of mixing in emulsion polymerizations. Figures 20–23 show the heat of reaction profile and the particle num-

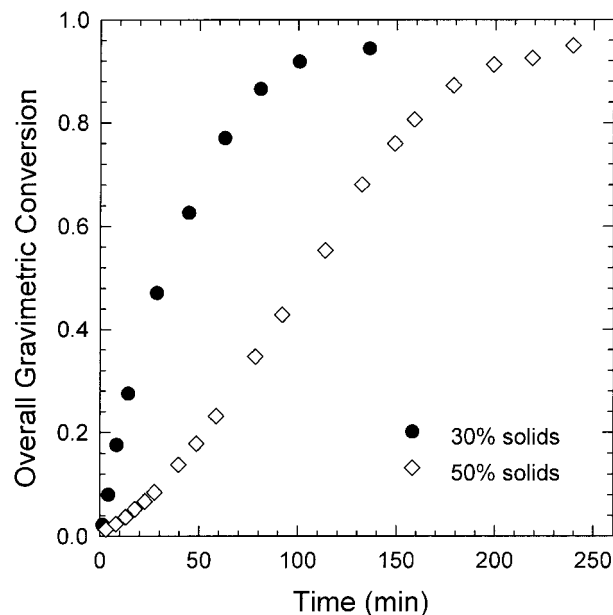


**Figure 21** Overall gravimetric conversion with respect to time as a function of solids content for the batch emulsion copolymerizations of styrene and *n*-butyl acrylate (1/1 weight ratio); 1000 rpm; A310 fluidfoil impeller;  $T_r = 70^\circ\text{C}$ .

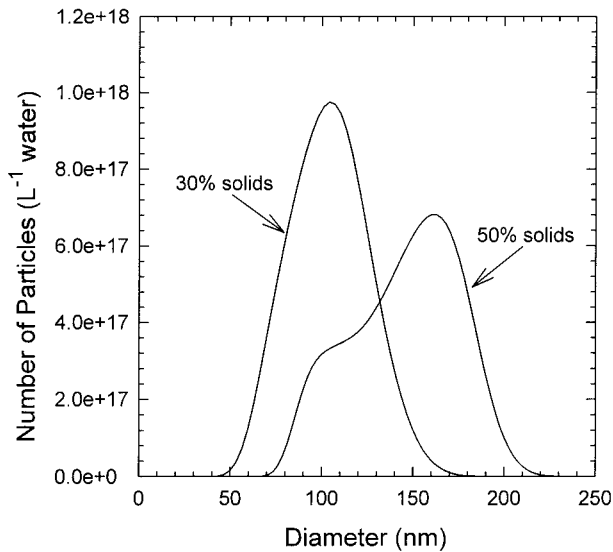


**Figure 22** Comparison of final latex particle size distributions for 30 and 50% solids content batch emulsion copolymerizations of styrene and *n*-butyl acrylate (1/1 weight ratio); 1000 rpm; A310 fluidfoil impeller;  $T_r = 70^\circ\text{C}$ .

ber evolution, overall gravimetric conversion, final latex particle size distribution, and copolymer composition, respectively, for the A310 fluidfoil impeller operated at 1000 rpm. The same profiles

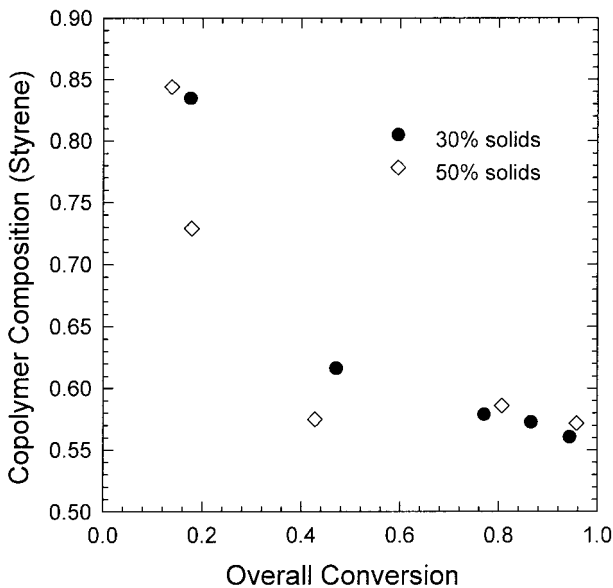


**Figure 23** Evolution of copolymer composition (molar) with respect to overall gravimetric conversion for 30 and 50% solids content batch emulsion copolymerizations of styrene and *n*-butyl acrylate (1/1 weight ratio); 1000 rpm; A310 fluidfoil impeller;  $T_r = 70^\circ\text{C}$ .

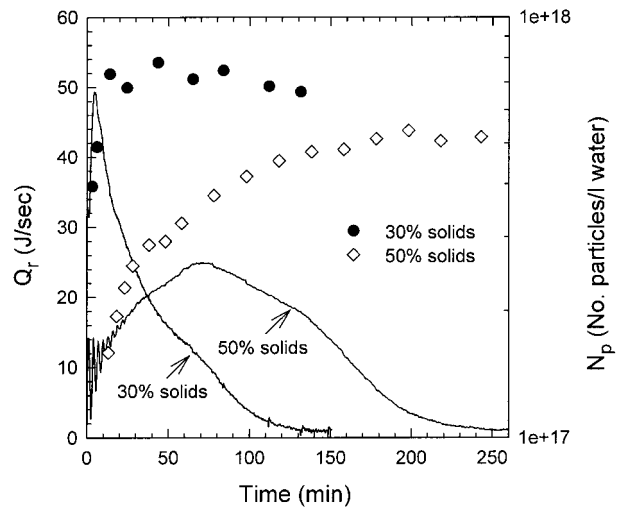


**Figure 24** Heat of reaction ( $Q_r$ , lines) and evolution of number of particles ( $N_p$ ,  $\bullet$ ,  $\diamond$ ) with respect to time as a function of solids content for the batch emulsion copolymerizations of styrene and *n*-butyl acrylate (1/1 weight ratio); 1000 rpm; Rushton impeller;  $T_r = 70^\circ\text{C}$ .

can be found in Figures 24–26 for the Rushton impeller (the copolymer composition was not determined in this case). For both impellers, the polymerizations carried out at 30% solids have faster rates compared to those at 50% solids (see

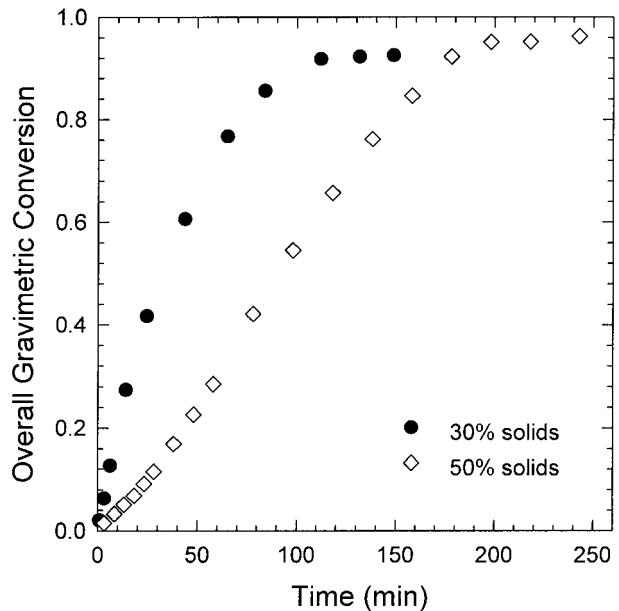


**Figure 25** Overall gravimetric conversion with respect to time as a function of solids content for the batch emulsion copolymerizations of styrene and *n*-butyl acrylate (1/1 weight ratio); 1000 rpm; Rushton impeller;  $T_r = 70^\circ\text{C}$ .

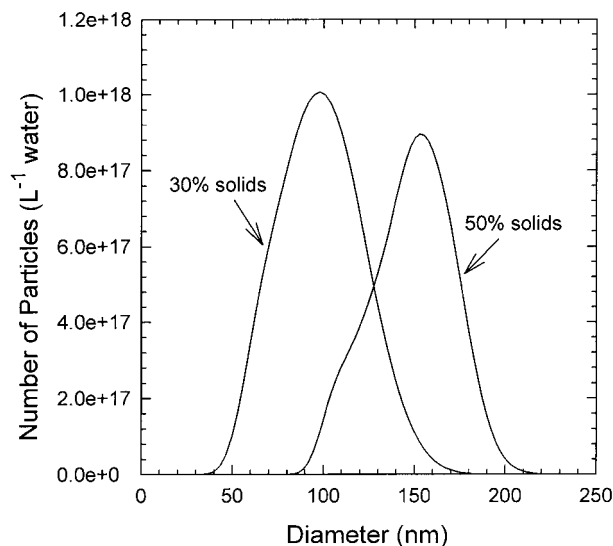


**Figure 26** Comparison of final latex particle size distributions for 30 and 50% solids content batch emulsion copolymerizations of styrene and *n*-butyl acrylate (1/1 weight ratio); 1000 rpm; Rushton impeller;  $T_r = 70^\circ\text{C}$ .

Fig. 20 and 24 for rate profiles and Fig. 21 and 25 for conversion profiles). If the surfactant did not partition between the oil and aqueous phases, one would expect a higher rate of polymerization at 50% solids since the emulsifier concentration is much higher ( $\sim 2.5$  times based on the aqueous phase). However, assuming that the partition coefficient is not a function of the monomer–water ratio, when one makes a material balance for the emulsifier, the amount of surfactant in the aqueous phase (using the data from our previous work)<sup>19</sup> prior to initiator addition would be slightly higher (4.47 mM) at 50% solids than that at 30% solids (3.87 mM). So one would expect the rates of polymerization to be similar at 30 and 50% solids contents. These very different results may be a consequence of one or both of the following: (1) more surfactant is associated with the oil phase at higher monomer–water ratios, leading to initially less free surfactant to be used in the nucleation of particles; and (2) the distribution of the chain lengths of the ethylene oxide groups of Triton X-405 in the aqueous phase is different at the 2 solids contents, leading to a much lower initial emulsifier concentration in the aqueous phase at 50% solids. (As alluded to earlier, Triton X-405 consists of surfactant molecules varying in chain length around an average of 40 ethylene oxide groups per molecule). Figures 20 and 24 also show that the final numbers of particles are similar for the 2 solids contents. When the final

particle size distributions are compared (see Fig. 22 and 26), it is seen that at the lower solids contents, unimodal latex particle size distributions are obtained, which is not the case at the higher solids. This again is likely to be due to more surfactant being associated initially with the oil phase for the higher solids, leading to free surfactant in the later stages of the polymerization, which is used partly for creating new particles. These results also raise questions about the nucleation mechanism(s) at 50% solids. It is possible that the initial conditions correspond to surfactant levels below the CMC, leading to homogeneous nucleation, followed by micellar nucleation, or perhaps both nucleation periods are mainly micellar. In addition, the solids content may also have an effect on the copolymer composition evolution with respect to conversion (Fig. 23), although the data presented are insufficient to come to a solid conclusion. All these results indicate that solids content is an important variable in studying the effect of mixing on the kinetics of emulsion polymerization.

## CONCLUSIONS

In this work, the role of mixing in emulsion copolymerizations of styrene and *n*-butyl acrylate was investigated. Based on the following evidence, it is concluded that solids content plays an important role in determining the effects of agitation speed and impeller type on the polymerization kinetics.

At 30% solids, as the impeller speed was increased from 400 to 1000 rpm, the initial number of particles and, thus, the initial rate of polymerization, decreased. This is due to the creation of a greater number of monomer droplets with correspondingly smaller sizes at the higher impeller speed, leading to the adsorption of more surfactant on the increased surface area of the monomer droplets with less surfactant being available in the aqueous phase for creating the initial particles. The total number of particles and the overall rate were not significantly affected by the impeller speed.

Comparison of the polymerizations using the A310 fluidfoil and Rushton impellers showed that the rates of polymerizations were not affected by the impeller type at 30% solids. There were slight differences in the numbers of particles, which could be attributable to experimental error. On the other hand, when the polymerizations carried

out at 50% solids were compared in terms of impeller type, it was observed that polymerizations ran using the A310 fluidfoil had a slower rate with a more distinct second population of particles compared to that using the Rushton impeller. This was explained by the mixing behavior of the A310 fluidfoil impeller. Although the A310 fluidfoil is supposed to be a relatively low shear impeller, due to its configuration in the reactor (that is, being relatively close to the wall of the reactor), it is believed that it creates more shear compared to the Rushton impeller. This results in more monomer droplets being formed, leading to more surfactant associated with them. As the droplets become depleted, more surfactant becomes available, some of which is used for the stabilization of the existing particles, while a portion of the remaining surfactant is used for creating new ones.

The effect of solids content is more pronounced than the effect of the other variables (that is, impeller type and speed) for the emulsion copolymerizations of styrene and *n*-butyl acrylate. Contrary to what was expected, polymerizations carried out at 50% solids had lower polymerization rates than those at 30% solids. In addition, the final latex particle size distributions were bimodal at 50% solids, whereas the 30% solids latexes had unimodal particle size distributions. These results were attributed to different partitioning behaviors of the surfactant between the oil and aqueous phases; as the monomer-to-water ratio increases, more surfactant partitions into the oil phase, leading to a lower amount in the aqueous phase, and/or the distribution of the surfactant chain lengths (ethylene oxide groups) in the aqueous phase varies with the monomer-to-water ratio. This results in a lower initial number of particles and, thus, the lower rate. Again, as the droplets are depleted, the surfactant becomes available in the aqueous phase, some of which is used for creating new particles.

The impeller speed, type, and solids content did not have any significant effects on the copolymer composition for the emulsion copolymerizations of styrene and *n*-butyl acrylate. The copolymer was richer in styrene in the earlier stages of the polymerization due to its higher reactivity ratio.

## REFERENCES

1. S. R. Scunmukham, V. L. Hallenbeck, and R. I. Guile, *J. Polym. Sci.*, **6**, 691 (1951).
2. C. J. Schoot, J. Baker, and K. H. Klassens, *J. Polym. Sci.*, **7**, 657 (1951).
3. S. Omi, Y. Shiraishi, H. Sato, and H. Kubota, *J. Chem. Eng. Jpn.*, **2**, 64 (1969).
4. M. Nomura, M. Harada, W. Eguchi, and S. Nagata, *J. Appl. Polym. Sci.*, **16**, 835 (1972).
5. A. L. Rollin, I. Patterson, J. Archambault, and P. Bataille, in *Polymerization Reactors and Processes*, J. N. Henderson and T. C. Bouton, Eds., ACS Symposium Series **104**, American Chemical Society, Washington, DC, 1979, p. 113.
6. L. Varela de la Rosa, M.S. thesis, Lehigh University, 1992.
7. C. P. Evans, P. M. Hay, L. Marker, R. W. Murray, and O. J. Sweeting, *J. Appl. Polym. Sci.*, **13**, 39 (1961).
8. R. Zollars, *J. Appl. Polym. Sci.*, **24**, 1353 (1979).
9. V. Stannett, A. Klein, and M. Litt, *Br. Polym. J.*, **7**, 139 (1975).
10. P. Bataille, J. F. Dalpe, F. Dubuc, and L. Lamoreux, *J. Appl. Polym. Sci.*, **39**, 1815 (1990).
11. P. A. Weerts, J. L. M. van der Loos, and A. L. German, *Makromol. Chem.*, **192**, 1993 (1991).
12. E. D. Sudol, in *Advances in Emulsion Polymerization and Latex Technology*, Lehigh University, Bethlehem, PA, 1997.
13. L. Varela de la Rosa, E. D. Sudol, M. S. El-Aasser, and A. Klein, *J. Polym. Sci., Part A: Polym. Chem.*, **34**, 461 (1996).
14. A. Urretabizkaia, E. D. Sudol, M. S. El-Aasser, and J. M. Asua, *J. Polym. Sci., Part A: Polym. Chem.*, **31**, 2907 (1993).
15. S. Omi, K. Kushibiki, M. Negishi, and M. Iso, *Zairyo Gijutsu*, **3**, 426 (1985).
16. L. Varela de la Rosa, Ph.D. dissertation, Lehigh University, 1996.
17. E. Özdeğer, E. D. Sudol, M. S. El-Aasser, and A. Klein, *J. Polym. Sci., Part A: Polym. Chem.*, **35**, 3813 (1997).
18. E. Özdeğer, E. D. Sudol, M. S. El-Aasser, and A. Klein, *J. Polym. Sci., Part A: Polym. Chem.*, **35**, 3827 (1997).
19. E. Özdeğer, E. D. Sudol, M. S. El-Aasser, and A. Klein, *J. Polym. Sci., Part A: Polym. Chem.*, **35**, 3837 (1997).